

Large anisotropy of spin polarization in Heusler alloy Ni₂MnGa induced by martensitic transformation

Z. Y. Zhu,^{a)} H. W. Zhang, S. F. Xu, J. L. Chen, Z. X. Cao, and G. H. Wu

Beijing National Laboratory for Condensed Matter Physics, Institute of Physics, Chinese Academy of Sciences, Beijing 100080, People's Republic of China

(Received 26 November 2007; accepted 5 March 2008; published online 5 May 2008)

Spin polarization both in the cubic austenitic and tetragonal martensitic phases of the Ni₂MnGa alloy has been investigated using first-principles calculations combined with classical Bloch–Boltzmann transport theory. It is shown that the degree of spin polarization, while decreasing from 42% in the ⟨001⟩ directions of the austenitic phase to 30% in the [100] direction of the martensitic phase, rises to 75% in the [001] direction of the martensitic phase, resulting from a preferential reconstruction of the spin-down Fermi surfaces upon martensitic transformation. With this finding, various recent intriguing electrical measurements upon Ni₂MnGa across the martensitic transformation can find an explanation. This also opens a way of searching for giant magnetoresistance materials. © 2008 American Institute of Physics. [DOI: 10.1063/1.2917406]

I. INTRODUCTION

Since the discovery of giant magnetoresistance (GMR) effect in multilayered Fe/Cr and Co/Cu structures,^{1–3} many research efforts have been devoted to further promoting the magnitude of GMR. One of the very effective routes is to increase the degree of spin polarization (DSP) of the ferromagnetic layers. As a crucial parameter in determining the magnitude of GMR, DSP characterizes the difference between the contributions of up spins and down spins to the electronic transport properties.⁴ With regard to DSP, the half-metals are obviously the optimum candidates since they exhibit a 100% spin polarization at absolute zero temperature. Unfortunately, however, only a few materials, such as NiMnSb, Co₂MnSi, CrO₂, and Fe₃O₄, have been identified as half-metals.^{5–8} So a natural question to consider is, whether it is possible to achieve a very large DSP in ordinary (non-half-metallic) materials via structure manipulation so as to extend the family of the GMR materials?

The Heusler alloy Ni₂MnGa is one of the well-known ferromagnetic shape memory alloys.^{9,10} At temperatures over 220 K, it displays a cubic structure with an $L2_1$ atomic ordering (space group $Fm\bar{3}m$), which can be viewed as four interpenetrating *fcc* sublattices occupied in sequence by Ni, Mn, Ni, and Ga atoms, respectively.⁹ Upon cooling, the high-temperature cubic polymorph, also termed the austenitic phase, undergoes a martensitic transformation into the tetragonal martensitic phase with $c/a \approx 0.94$.⁹ This is a diffusionless, first order transition from the austenitic parent phase of higher symmetry to the martensitic phase of lower symmetry. Considering also the ferromagnetism of the martensitic phase, the Ni–Mn–Ga alloys are bestowed with many applicable properties beyond the shape memory effect.^{10,11} In this article, we report the computation of the DSP for both the austenitic and martensitic phases of Ni₂MnGa using first-principles calculations combined with classical Bloch–

Boltzmann transport theory. It is found that following the martensitic transformation, the DSP of this alloy decreases from 42% to 30% in the [100] direction, whereas it increases from 42% to 75% in the [001] direction (specified with regard to the tetragonal martensitic phase). An asymmetrical effect of the lattice distortion upon the Fermi surface topology, consequently the electronic mobility, of up spins and down spins should be responsible for the extraordinary enhancement of DSP in a certain lattice direction.

II. CALCULATION DETAIL

Different definitions of DSP have been adopted for the discussion of various spin dependent transport behaviors.¹² For spin-polarized photoemission, it is the number of conduction electrons that uniquely determines the magnitude of resistivity, so a “DOS” definition for DSP, i.e., the N definition in Ref. 12, is appropriate. In contrast, the GMR effect is also affected by the velocity of the conduction electrons, therefore the difference in the velocities of the spin-up and spin-down conduction electrons has to be taken into account in the DSP definition for the relevant discussions. Accordingly, we adopt the σ -definition for DSP, i.e., the Nv^2 definition in Ref. 12, which is written as

$$P_{ii} = \frac{\sigma_{ii}(\uparrow) - \sigma_{ii}(\downarrow)}{\sigma_{ii}(\uparrow) + \sigma_{ii}(\downarrow)}. \quad (1)$$

Here, $\sigma_{ii}(\uparrow)$ and $\sigma_{ii}(\downarrow)$ denote the i direction conductivities of up spins and down spins, respectively. Following the classical Bloch–Boltzmann transport theory with the relaxation time approach,¹³ spin dependent conductivity in the i direction, $\sigma_{ii}(m)$ ($m = \uparrow$ or \downarrow for up spins or down spins), is given by

^{a)}Electronic mail: zyzhu@aphy.iphy.ac.cn.

$$\sigma_{ii}(m) \propto \sum_{m,n} \int \tau(\mathbf{k}, m, n) v_{m,n}^i(\mathbf{k}) v_{m,n}^j(\mathbf{k}) \delta[\varepsilon_{m,n}(\mathbf{k}) - E_F] d^3\mathbf{k}. \quad (2)$$

Here, m and n are the spin and band index, v_n^i denotes the projection of the electron velocity on the i direction, ε_n is the band energy, E_F is the Fermi energy, and τ is the relaxation time. Remarkably, v_n^i , ε_n , and E_F are all related to the electronic band structure and can be rigorously evaluated from the first-principles calculations. In contrast, the relaxation time τ that arises from the scattering of electrons by defects or interfaces is difficult to be determined theoretically for the time being. The conductivity specified in Eq. (2) relies upon both the various possible scattering mechanisms and the “pure band effect,” as is in the case of GMR effect where the impact of the spin dependent electron scattering¹⁴ as well as of the electronic structure for the ideal lattice¹⁵ has been confirmed. In the following discussion, we adopt a constant relaxation time approximation,¹⁶ focusing our attention on the effect of the electronic structure. Although the detailed features of the scattering process have been smeared out, it will be shown that the calculated conductivity for Ni₂MnGa agrees well with several experimental measurements.

To compute the spin-polarized electronic band structure for the cubic austenitic and tetragonal martensitic phases of Ni₂MnGa, we employed the self-consistent full-potential linearized-augmented plane-wave method based on the local spin-density approximation within the density functional theory.¹⁷ The lattice constants for the unit cell, which contains eight Ni, four Mn, and four Ga atoms, are $a=5.825$ Å for the cubic phase and $a=5.92$ Å, $c=5.566$ Å for the tetragonal phase.⁹ The self-consistency was achieved at 20 k -points for the cubic phase and 40 k -points for the tetragonal phase in each irreducible Brillouin zone. A cutoff energy was set at 350 eV for all the calculations. For the summation over the electronic states in Eq. (2), the first Brillouin zone was divided into a mesh of 27000 k -points, which suffices to achieve an accuracy of a few percents.

III. RESULTS AND DISCUSSION

The DSP of Ni₂MnGa in the cubic austenitic phase amounts to 42% in the highly symmetric $\langle 001 \rangle$ directions, in the tetragonal martensitic phase it diverges into two distinct values due to the lowered symmetry. It decreases to 30% in the [100] direction but measures as high as 75% in the [001] direction, i.e., the spin polarization is significantly enhanced along the c axis.

In order to explain this unexpected result, the contribution of each individual conduction band to the conductivities of the up spins and down spins, as exemplified in Fig. 1, has to be closely inspected. Upon martensitic transformation, the conductivities of the up spins and down spins are modified quite differently. With regard to that in the $\langle 001 \rangle$ directions of the austenitic phase, the conductivities of up spins, both in the [100] and in the [001] directions, only slightly change, and in an irregular way, leading to a decrease of only 2% in the total conductivity. On the contrary, the conductivity of the down spins generally (except for the bands 55 and 56)

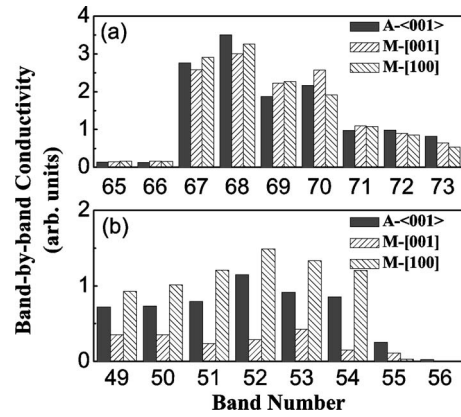


FIG. 1. Band-by-band contribution of spin-up (a) and spin-down (b) conduction bands to the total conductivity in the Ni₂MnGa alloy. Here, “A” stands for austenitic phase and “M” for martensitic phase, respectively.

displays a significant drop in the [001] direction but increases a lot in the [100] direction. In fact, the total conductivity of down spins suffers a loss of 65% in the [001] direction while it increases for 31% in the [100] direction. This clearly indicates an opposite change in the DSPs in the [100] direction and in the [001] direction. Accordingly, from Eq. (1), the DSP changes, as specified in the last section, from 42% for the austenitic phase in the $\langle 001 \rangle$ directions, to a value of 30% in the [100] direction and a value of 75% in the [001] direction of the martensitic phase.

The calculation results presented above agree well with the experimental results of conductivity measurements on Ni₂MnGa alloys. According to the band-by-band conductivity given in Fig. 1, the total conductivities in the [001] and [100] directions of the tetragonal martensite, normalized to that in the $\langle 001 \rangle$ directions for the cubic austenitic phase, should be 0.81 and 1.08, respectively. This predicts a considerable crystallographic anisotropy of conductivity in the Ni₂MnGa martensite, i.e., $\sigma_{M,[001]}=0.75\sigma_{M,[100]}$. Recently, Srivastava *et al.* succeeded in preparing a single variant phase (c -oriented) of martensitic Ni₄₉Mn₂₉Ga₂₂, and measured an “appreciable” anisotropy in the conductivity $\sigma_{c||l} < \sigma_{c\perp l}$.¹⁸ The failure to obtain a quantitative evaluation of the conductivity anisotropy for Ni₂MnGa martensite lies in the difficulty of preparing a single-crystal sample. The martensite derived from the single-crystal austenitic phase upon martensitic transformation is generally polyvariant due to the simultaneous occurrence of the various martensitic variants (up to 24). For such a polyvariant Ni₂MnGa sample, supposing the c axes of its 24 martensitic variants are equiprobably distributed in all directions, then its conductivity is only about 3% less than the austenitic phase. This, when reflected on the R - T curve, will display a small hump at around the transformation temperature, as was confirmed by our measurement, see Fig. 2, and by other researches.¹⁹

One of the most meaningful conclusions drawn from the above calculations is that the DSP of Ni₂MnGa can be enormously changed via the martensitic transformation, and a significantly enhanced value can be found in the [001] direction of the martensite. Two questions can be posed here. First, why was the change in the conductivity for most spin-down bands much larger than that for the spin-up bands.

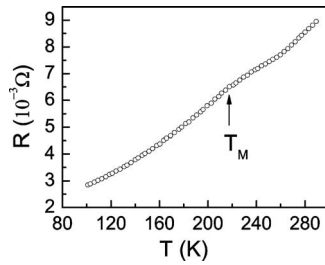


FIG. 2. Temperature dependence of the resistance of Ni_2MnGa measured in the heating run. T_M stands for the critical temperature for reversed martensitic transformation.

Second, why did the conductivity for down spins increase in the $[100]$ direction while it more seriously drops in the $[001]$ direction? To find a reasonable answer to these questions, we made a close inspection of the electronic band structures of the two phases (Fig. 3). From the results of DOS (not shown here), it can be found that near the Fermi level there is no obvious difference between the up-spin DOS of both phases, whereas a peak of the down-spin DOS splits upon the martensitic transformation (shifted for ~ 0.18 eV). This is in good agreement with the results reported in Ref. 20, in which this peak splitting is considered as an indication of the band Jahn–Teller effect that causes the martensitic transformation of Ni_2MnGa .

The spin-polarized band structures near the Fermi level for both phases are plotted in Fig. 3. For the cubic austenitic phase, nine spin-up bands (65–73) and eight spin-down bands (49–56) run across the Fermi level. However, for the tetragonal martensitic phase, the spin-down band 56 rises and fails to meet the Fermi level, hence only seven spin-down bands remain running across the Fermi level. By comparing the fine structure of the bands for both phases, it can be seen that the martensitic transformation has little effect on the spin-up bands, whereas the spin-down band structure is rather remarkably modified along some k -paths where a band that crosses, or misses, the Fermi level in the cubic austenitic phase turns to depart from, or run across, the Fermi level in the tetragonal martensitic phase. In fact, this observation is in accordance with the DOS peak splitting near the Fermi level for the down spins. Therefore, both DOS and the fine band

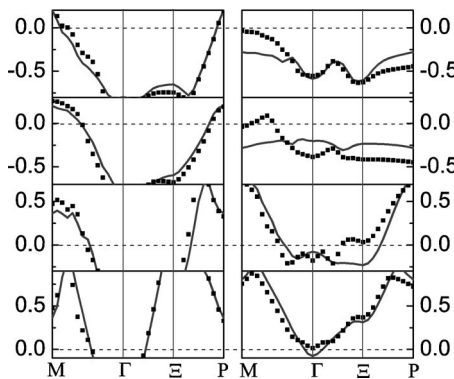


FIG. 3. Energy bands along three characteristic k -paths for Ni_2MnGa in the austenitic phase (solid line) and martensitic phase (scattered line). Here illustrated, from top to bottom, are four spin-up bands 66, 68, 70, and 72 (left), and four spin-down bands 50, 52, 54 and 56 (right). The horizontal dashed lines indicate the Fermi levels.

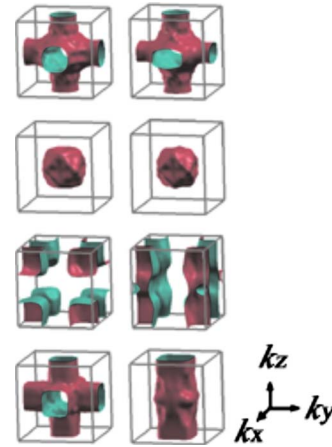


FIG. 4. (Color online) Characteristic Fermi surface sheets for the spin-up bands 70 and 72 as well as the spin-down bands 52 and 54 in the unit cell of Ni_2MnGa (from top to bottom). Left column: cubic austenitic phase. Right column: tetragonal martensitic phase.

structure have indicated a preferential influence on the conduction bands of down-spins by phase transition.

Nevertheless, the band structures given in Fig. 3 illustrate only the electronic energy on a few k -paths of high symmetry. It would be desirable to depict the Fermi surface sheet for each conduction band in the first Brillouin zone so as to more straightforwardly demonstrate the properties of the conduction electrons. Using the XCRYSDEN program,²¹ the Fermi surface sheets of all the conduction bands have been plotted for the austenitic and the martensitic phases, with some exemplified in Fig. 4. It can be seen that the martensitic transformation leads to only very tiny modification to the Fermi surface topology for up spins, whereas for down spins the Fermi surface sheets generally are remarkably deformed. The characteristic change of the Fermi surface sheets for spin-up bands, except for bands 65–69 and 71 and 72 which remain nearly intact, is the tendency that the two pieces of the Fermi surface with $k_z > 0$ and $k_z < 0$ approach mutually to each other along k_z -direction due to the martensitic transformation. For spin-down bands, this tendency of mutual approaching is so obvious that pieces of some Fermi surfaces merge together and even then disappear following the transition. The Fermi surface sheets of spin-down bands 51–54 are reconstructed into a nearly cylindrical shape with its axis along the k_z direction, and the Fermi surface sheets of 56 spin-down band digress away from the Fermi surface, thus, making no contribution to conduction.

The effect of the deformed Fermi surface is twofold. On one hand, the shrinkage of the Fermi surface leads to a reduced DOS at the Fermi level, consequently, a decreased amount of conduction electrons. On the other hand, it induces a redistribution of the velocities for the conduction electrons. As pointed out in Ref. 15, the Fermi velocity is normal to the Fermi surface since the velocity of a conduction electron is proportional to the band energy gradient in the reciprocal space. Thus, providing an ideally cylindrical Fermi surface sheet, the velocity of the conduction electron will lie in the k_x - k_y plane, having a vanishing component in

the k_z direction. This is to say that the more the Fermi surface sheets mimic a perfect cylinder, the larger the anisotropy in velocity for the conduction electrons.

Now the answers to the two questions we previously posed become clear. First, the almost unchanged Fermi surface of spin-up bands leads to an almost unchanged conductivity for up spins, whereas the reconstruction of the Fermi surfaces of the most spin-down bands results in great change in both the DOS at Fermi level and the velocity of the conduction electrons, hence the conductivity. Second, the reconstruction of nearly all the Fermi surface sheets of spin-down electrons into a nearly cylindrical shape leads to a strongly increased x - y component and a much reduced z component of the electronic velocity, therefore an obvious increase of conductivity of down spins in [100] direction and a great decrease in [001] direction are observed. Moreover, the reconstruction of the Fermi surface, especially the partially disappearing or even completely vanishing of some surface sheets, leads to a decrease of minority DOS at Fermi level by about 17%. Decreased DOS, i.e., decreased number of conduction electrons, equally contributes to the conductivity change of down spins both in the [001] direction and in the [100] direction. This is just the reason why the amplitude of the increase in conductivity of down spins in the [100] direction is smaller than that of the decrease in the [001] direction. So far, from the above discussion, it has been recognized that the significantly elevated DSP in the [001] direction of Ni_2MnGa following the martensitic transformation is the result of an almost unchanged Fermi surface topology of up spins and the reconstruction of the Fermi surface of down spins. A more straightforward view can be provided by inspecting the spatial distribution of the electron density for different conduction bands. From the calculations, we see that the conduction electrons are dominantly distributed around the Ni atoms, and the electronic cloud manifests a totally different spatial extension for spin-up and spin-down conduction bands. In the former case, the electronic cloud concentrates in between the principal axes (of the lattice), whereas in the latter case it mainly spreads along the principal axes. Therefore the spin-down bands are more liable to the cubic-tetragonal structural transition.

IV. CONCLUSION

In summary, DSP in the sense of the σ -definition, taking into account the influence of the electronic structure, has been computed for the cubic austenitic phase and tetragonal martensitic phase of the stoichiometric Ni_2MnGa alloy. It changes from the value of 42% for the austenitic phase in the $\langle 100 \rangle$ directions, to a value of 30% in the [100] direction and to a significantly increased value of 75% in the [001] direction for the martensitic phase. This largely enhanced DSP in

the [001] direction of the martensitic phase is a result of the almost unchanged Fermi surface topology of up spins and the reconstruction of Fermi surface of down-spins into nearly cylindrical shapes. Here, the introduction of the electronic velocity for the description of spin dependent transport properties associates the DSP of a material to its Fermi surface topology. The preferential influence of the martensitic transformation upon the Fermi surface topology of the down spins is a consequence of the much larger DOS value for minority spin (down spin here) at the Fermi level. This means that a much higher DSP may be obtained via a structural transition that deforms the sample along a certain lattice direction, provided a much larger value of minority spin DOS at the Fermi level is initiated. This provides a clue to the search for GMR candidate materials in those substances that may undergo structural phase transition or be liable to lattice distortion under external stresses.

ACKNOWLEDGMENTS

This work was supported by the National Natural Science Foundation of China Grant No. 50571113.

- ¹M. N. Baibich, J. M. Broto, A. Fert, F. Nguyen Van Dau, F. Petroff, P. Eitenne, G. Creuzet, A. Friederich, and J. Chazelas, *Phys. Rev. Lett.* **61**, 2472 (1988).
- ²G. Binasch, P. Grünberg, F. Saurenbach, and W. Zinn, *Phys. Rev. B* **39**, 4828 (1989).
- ³S. S. P. Parkin, R. Bhadra, and K. P. Roche, *Phys. Rev. Lett.* **66**, 2152 (1991).
- ⁴J. F. Gregg, I. Petej, E. Jouguelet, and C. Dennis, *J. Phys. D* **35**, R121 (2002).
- ⁵R. A. de Groot, F. M. Mueller, P. G. van Engen, and K. H. J. Buschow, *Phys. Rev. Lett.* **50**, 2024 (1983).
- ⁶S. Ishida, T. Masaki, S. Fujii, and S. Asano, *Physica B* **245**, 1 (1998).
- ⁷K. Schwarz, *J. Phys. F: Met. Phys.* **16**, L211 (1986).
- ⁸A. Yanase and K. Siratori, *J. Phys. Soc. Jpn.* **53**, 312 (1984).
- ⁹P. J. Webster, K. R. A. Ziebeck, S. L. Town, and M. S. Peak, *Philos. Mag. B* **49**, 295 (1984).
- ¹⁰K. Ullakko, J. K. Huang, C. Kantner, R. C. O'Handley, and V. V. Kokorin, *Appl. Phys. Lett.* **69**, 1966 (1996).
- ¹¹G. H. Wu, C. H. Yu, L. Q. Meng, J. L. Chen, F. M. Yang, S. R. Qi, W. S. Zhan, Z. Wang, Y. F. Zheng, and L. C. Zhao, *Appl. Phys. Lett.* **75**, 2990 (1999).
- ¹²I. I. Mazin, *Phys. Rev. Lett.* **83**, 1427 (1999).
- ¹³J. M. Ziman, *Electrons and Phonons* (Oxford University Press, London, 1967), Chap. VII.
- ¹⁴P. M. Levy, S. F. Zhang, and A. Fert, *Phys. Rev. Lett.* **65**, 1643 (1990).
- ¹⁵V. N. Antonov, A. Ya. Perlov, P. M. Oppeneer, A. N. Yaresko, and S. V. Halilov, *Phys. Rev. Lett.* **77**, 5253 (1996).
- ¹⁶J. Ziman, *Principles of the Theory of Solids* (Cambridge University Press, Cambridge, England, 1964).
- ¹⁷E. Wimmer, H. Krakauer, M. Weinert, and A. J. Freeman, *Phys. Rev. B* **24**, 864 (1981).
- ¹⁸V. K. Srivastava, R. Chatterjee, and R. C. O'Handley, *Appl. Phys. Lett.* **89**, 222107 (2006).
- ¹⁹F. Zuo, X. Su, P. Zhang, G. C. Alexandrakis, F. Yang, and K. H. Wu, *J. Phys.: Condens. Matter* **11**, 2821 (1999).
- ²⁰S. Fujii, S. Ishida, and S. Asano, *J. Phys. Soc. Jpn.* **58**, 3657 (1989).
- ²¹A. Kokalj, *J. Mol. Graphics Modell.* **17**, 176 (1999).